Proceedings of the Online Conference "Applications of Physics in Mechanical and Material Engineering"

Magnetisation Process of $Fe_{61+x}Co_{10-x}Y_8W_1B_{20}$ Bulk Amorphous Alloys

P. Sikora[a], M. Nabiałek[b], K. Błoch[b], J. Gondro[b], A.V. Sandu[c,d], M.M.A.B. Abdullah[d], A. Kalwik[a], P. Mousavi[e], S. Hasani[e] and B. Jeż[b]

[a] *Department of Technology and Automation, Faculty of Mechanical Engineering and Computer Science, Częstochowa University of Technology, al. Armii Krajowej 19, 42-200 Częstochowa*
[b] *Department of Physics, Częstochowa University of Technology, al. Armii Krajowej 19, 42-200 Częstochowa, Poland*
[c] *Gheorghe Asachi Technical University of Iasi, Faculty of Materials Science and Engineering, Blvd. D. Mangeron 41, 700050, Iasi, Romania*
[d] *Center of Excellence Geopolymer & Green Technology (CEGeoGTech), School of Materials Engineering, Universiti Malaysia Perlis, 01000 Kangar, Perlis, Malaysia*
[e] *Department of Mining and Metallurgical Engineering, Yazd University, 89195-741, Yazd, Iran*

Doi: 10.12693/APhysPolA.139.582 *e-mail: bartek199.91@o2.pl

Generally speaking, the structure of amorphous alloys can be difficult to describe accurately. The absence of repeating arrangements of atoms within the volume of the alloy generates unique material properties, but at the same time makes it difficult to describe the structure systematically. One of the exceptions to this rule is the class of amorphous alloys that exhibit ferromagnetic properties. The structure of these alloys can be assessed, in an indirect way, using the sensitivity of the magnetisation vector to any inhomogeneities in their volume. This paper presents the results of indirect structural research in accordance with the assumptions of H. Kronmüller's theory. The $Fe_{61+x}Co_{10-x}Y_8W_1B_{20}$ alloys — with variable Co and Fe content— were investigated. The alloy samples were made using the injection-casting method. The structure of each of the produced materials was investigated using X-ray diffraction and by examining indirectly the course of the magnetisation process in the area known as the approach to ferromagnetic saturation. In the case of the tested alloys, it was found that the magnetisation process is related to the rotation of the magnetisation vector around linear defects.

topics: rapidly-quenched alloys, X-ray diffractometry, soft magnetic materials, injection-casting method, approach to ferromagnetic saturation

1. Introduction

Amorphous ferromagnetic alloys that are based on the Fe matrix show the so-called soft magnetic properties, i.e., a high value of saturation magnetisation and magnetic susceptibility as well as a low value of the coercive field. Soft magnetic properties are characteristic of classic amorphous alloys with a high content of Fe and Co [1–4]. In the case of bulk amorphous alloys, achieving soft magnetic properties is much more difficult due to the necessity to reduce the content of ferromagnetic elements, replacing them partially with other transition metals and glass-forming elements such as B, P or C [6, 7]. Such soft magnetic properties are demonstrated, inter alia, by alloys based on Fe-Me-B systems [8, 9].

Structural defects have a significant influence on the magnetic properties of amorphous alloys. These defects take the form of free volumes (point defects) and pseudo-dislocation dipoles (linear defects) [10, 11]. The magnetisation vector is extremely sensitive to any inhomogeneities. In the vicinity of structural defects, the magnetisation vector is deviated, which results in a non-linear increase in magnetisation with increasing intensity of the external magnetic field. This fact can be used indirectly to give an assessment of structural defects through the analysis of primary magnetisation curves, in accordance with the assumptions of H. Kronmüller's theory [10, 12–14].

The aim of this study was to evaluate the effect of Fe and Co content on the nature of defects occurring in the structure of amorphous alloys with the formula $Fe_{61+x}Co_{10-x}Y_8W_1B_{20}$, and on the magnetic properties of the same tested alloys.

2. Materials and methods

Polycrystalline alloys with the composition $Fe_{61+x}Co_{10-x}Y_8W_1B_{20}$ (where $x = 0$ or 2) were produced by the arc method. The smelting process was carried out on a water-cooled copper plate. In each case, the alloy was melted using a non-consumable tungsten electrode at a current of 180–380 A. Each alloy was re-melted five times, with the ingot being inverted each time. The whole process was carried out under a protective atmosphere, after previously attaining a high vacuum. The resulting ingots were used to produce rapidly-cooled alloy samples by application of the injection casting method. Cleaned pieces of each required alloy were melted in a quartz crucible placed within a copper coil. The liquid melt was injected into water-cooled copper moulds. Rods were produced with a diameter of 1 mm and a length of 10 mm. The production process was carried out under a protective argon atmosphere.

X-ray diffraction (Bruker D8 Advance) was used to study the structure of each alloy. The diffractometer was equipped with a CuK_α lamp. Measurements were carried out in the range of 2θ angle from 30–100°, with a measuring step of 0.02° and an exposure time of 5 s.

Primary magnetisation curves and static magnetic hysteresis loops were recorded using a LakeShore vibration magnetometer. This research was carried out in the range of external magnetic field of up to 2 T. The primary magnetisation curves were analysed according to the theory of H. Kronmüller. It was assumed that the magnetisation can be described by the relationship:

$$\mu_0 M(H) = b\,(\mu_0 H)^{\frac{1}{2}} + \mu_0 M_s - \mu_0 M_s \left(\frac{a_{\frac{1}{2}}}{(\mu_0 H)^{\frac{1}{2}}} + \frac{a_1}{(\mu_0 H)^1} + \frac{a_2}{(\mu_0 H)^2} \right), \quad (1)$$

where M_s is the spontaneous magnetisation, μ_0 — the magnetic permeability of a vacuum, H — the magnetic field, a_i — the angular coefficients of the linear fit corresponding to the free volume and linear defects, b — the slope of the linear fit corresponding to the thermally-induced suppression of spin-waves by a magnetic field of high intensity.

Factors $a_{1/2}$, a_1, a_2, respectively, correspond to point defects, linear defects satisfying the relationship $D_{dip} < l_H$, and linear defects meeting the relationship $D_{dip} > l_H$, where D_{dip} is the width of the pseudodislocation dipole and l_H is the exchange distance. In strong magnetic fields, magnetisation is associated with the attenuation of thermally-excited spin-waves. This phenomenon is called the Holstein–Primakoff paraprocess [10] and is described by the spin-wave stiffness parameter D_{spf}. This parameter can be determined from the relationship:

$$b = 3.54\mu_0 \left(\frac{g\mu_B}{4\pi D_{spf}} \right)^{3/2} k_B T, \quad (2)$$

where k_B is the Boltzmann constant, μ_B — the Bohr magneton, g — the gyromagnetic factor and T — the temperature.

3. Results

Figure 1 shows the X-ray diffraction patterns measured for the produced alloys. The diffraction patterns show wide fuzzy maxima, originating from X-rays reflected from chaotically arranged atoms within the volume of the alloy. Such diffractograms are typical for amorphous materials. Figure 2 shows static magnetic hysteresis loops for the produced alloy samples. The $Fe_{61}Co_{10}Y_8W_1B_{20}$ alloy is characterised by a saturation magnetisation value $M_s = 1.09$ T, and a coercive field value $H_C = 18$ A/m. In the case of the $Fe_{63}Co_8Y_8W_1B_{20}$ alloy, the following values were determined $M_s = 1.11$ T and $H_C = 70$ A/m.

Analysis of the primary magnetisation curves for the tested alloys is presented in Figs. 3 and 4. Within the range of external magnetic field intensity from 0.03 to 0.05 T, the magnetisation process of the $Fe_{61}Co_{10}Y_8W_1B_{20}$ alloy is associated with the rotation of the magnetisation vector around point defects. In the range of magnetic field strength of 0.05–0.28 T, the magnetisation of the alloy is

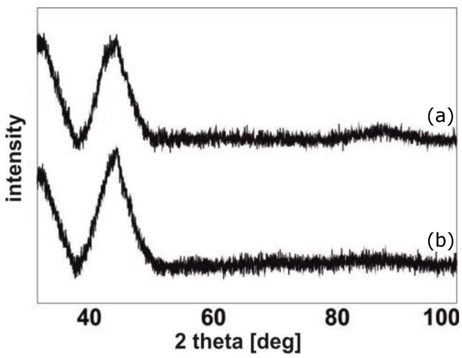

Fig. 1. X-ray diffraction patterns for the alloy samples: (a) $Fe_{61}Co_{10}Y_8W_1B_{20}$, (b) $Fe_{63}Co_8Y_8W_1B_{20}$.

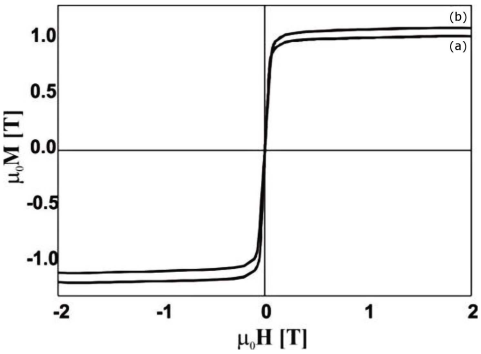

Fig. 2. Static magnetic hysteresis loops for the alloys: (a) $Fe_{61}Co_{10}Y_8W_1B_{20}$, (b) $Fe_{63}Co_8Y_8W_1B_{20}$.

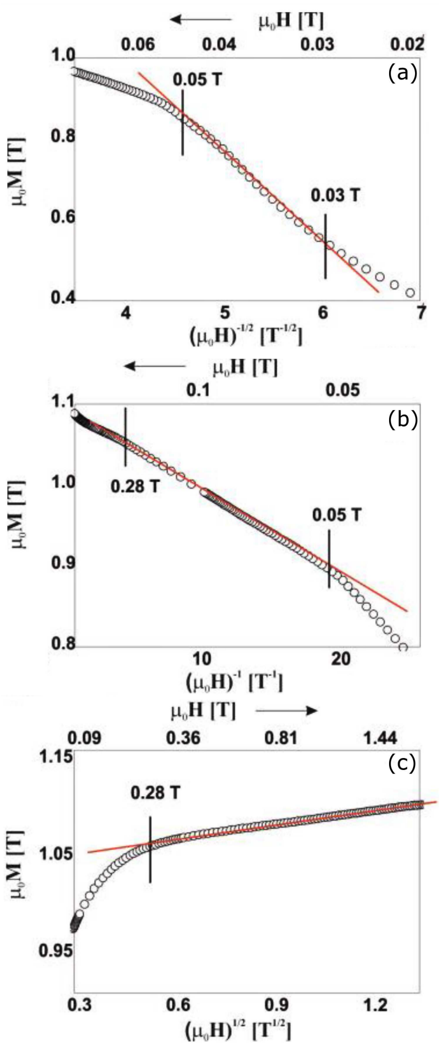

Fig. 3. Magnetisation of the $Fe_{61}Co_{10}Y_8W_1B_{20}$ alloy, as a function of: (a) $(\mu_0 H)^{-2}$, (b) $(\mu_0 H)^{1/2}$.

associated with linear defects that satisfy the relationship $D_{\rm dip} < l_H$. Above this area, a slight change in magnetisation is related to the attenuation of thermally-excited spin-waves [15, 16].

In the case of the $Fe_{63}Co_8Y_8W_1B_{20}$ alloy, the magnetisation process in strong magnetic fields is related to the rotation of the magnetisation vector around linear defects, whose widths are less than the exchange distance $D_{\rm dip} < l_H$. The Holstein–Primakoff paraprocess occurs in a magnetic field which is greater than 0.33 T. Based on the coefficient b, the value of the $D_{\rm spf}$ parameter was determined for each alloy: 40 meV nm^2 for the $Fe_{61}Co_{10}Y_8W_1B_{20}$ alloy and 44.9 meV nm^2 for $Fe_{63}Co_8Y_8W_1B_{20}$.

4. Conclusions

This paper presents the results of research on the structural and magnetic properties of bulk amorphous alloys that are based on the Fe matrix. Indirect structural examination showed that, in the volume of the $Fe_{61}Co_{10}Y_8W_1B_{20}$ alloy, there are point

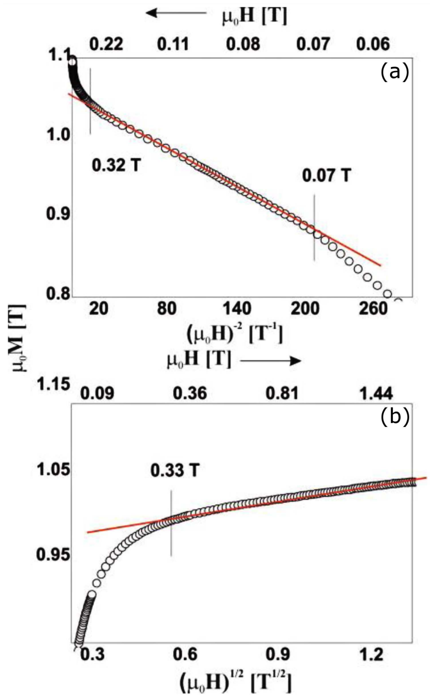

Fig. 4. Magnetisation of the $Fe_{63}Co_8Y_8W_1B_{20}$ alloy, as a function of: (a) $(\mu_0 H)^{-2}$, (b) $(\mu_0 H)^{1/2}$.

defects and linear defects with dimensions not exceeding the exchange distance. The structure of the $Fe_{63}Co_8Y_8W_1B_{20}$ alloy is dominated by pseudodislocation dipoles with dimensions exceeding the exchange distance. Structural defects have a key impact on the creation of the soft magnetic properties of the tested alloys. The presence of defects with smaller dimensions results in a much lower value of the coercive field than in the case of the alloy where the presence of defects meeting the relationship $D_{\rm dip} < l_H$ was identified. A smaller size of defects improves the exchange interactions, which facilitates the process of magnetisation. The higher magnetisation value of the $Fe_{63}Co_8Y_8W_1B_{20}$ alloy is related to the higher content of Fe atoms. The increase in the $D_{\rm spf}$ parameter, with the increase in magnetisation, suggests a lack of antiferromagnetic order in the studied alloys.

References

[1] M.E. Mchenry, M.A. Willard, D.E. Laughlin, *Prog. Mater. Sci.* **44**, 291 (1999).

[2] Y. Han, C.T. Chang, S.L. Zhu, A. Inoue, D.V. Louzguine-Luzgin, E. Shalaan, F. Al-Marzouki, *Intermetallics* **54**, 169 (2014).

[3] Y. Han, J. Ding, F.L. Kong, A. Inoue, S.L. Zhu, Z. Wang, E. Shalaan, F. Al-Marzouki, *J. Alloys Compd.* **691**, 364 (2017).

[4] Y. Han, A. Inoue, F.L. Kong, C.T. Chang, S.L. Shu, E. Shalaan, F. Al-Marzouki, *J. Alloys Compd.* **657**, 237 (2016).

[5] W.H. Wang, *Prog. Mater. Sci.* **52**, 540 (2007).

[6] S. Hasani, P. Rezaei-Shahreza, A. Seifoddini, M. Hakimi, *J. Non-Cryst. Solids* **497**, 40 (2018).

[7] P. Rezaei-Shahreza, A. Seifoddini, S. Hasani, *J. Non-Cryst. Solids* **471**, 286 (2017).

[8] K. Jeż, M. Nabiałek, S. Walters, A.V. Sandu, B. Jeż, *Acta Phys. Pol. A* **138**, 196 (2020).

[9] B. Jeż, J. Wysłocki, S. Walters, P. Postawa, M. Nabiałek, *Materials* **13**, 1367 (2020).

[10] H. Kronmüller, S. Parkin, *Handbook of Magnetism and Advanced Magnetic Materials*, Wiley, Hoboken (NJ) 2007.

[11] P. Vizureanu, *Metal. Int.* **14**, 5 (2009).

[12] H. Grimm, H. Kronmüller, *Phys. Status Solidi B* **117**, 663 (1983).

[13] H. Kronmüller, M. Fähnle, *Micromagnetism and the Microstructure of Ferromagnetic Solids*, Cambridge University Press, Cambridge 2003.

[14] T. Holstein, H. Primakoff, *Phys. Rev.* **59**, 388 (1941).

[15] J. Gondro, K. Błoch, M. Nabiałek, S. Garus, *Mater. Tehnol.* **50**, 559 (2016).

[16] K. Błoch, *Rev. de Chim.* **69**, 982 (2018).